Nanopatterning and plasmonic properties of plasma sputtered gold on diatom frustules

Julien Romann and Mari-Ann Einarsrud*
Department of Material Science and Engineering
Norwegian University of Science and Technology, NO-7491 Trondheim - NORWAY

ABSTRACT

Bio-silica nanostructures from diatoms (called frustules) featuring plasmonic gold nanoparticles (NPs) are elaborated using two methods based on plasma sputtering of gold. The first investigated method uses a thermal treatment to induce the thermal dewetting of a plasma sputtered gold layer on the diatom frustules. The second method first consists of coating the frustules with polyethylene glycol before sputtering gold on these frustules. For both methods, the amount of gold appears to be a key parameter regarding the final obtained layer, which can either be nanostructured by cavities or consist in individual gold NPs. For an amount of sputtered gold equivalent to form a 5 nm thick layer, both methods allow obtaining diatom frustules covered by gold NPs with a size around 20 nm and a narrow size distribution. The UV-visible characterization of the diatom frustules featuring gold NPs highlights a plasmon extinction band in agreement with individual gold NPs with a size below 25 nm.

INTRODUCTION

The plasmonic properties of noble metal nanoparticles (NPs) have been subject to widespread interest in recent years [1-9]. Many promising applications involving local surface plasmon resonance (LSPR) still drive a strong research activity in this area. More recently, the elaboration of plasmonic systems combining noble metal NPs and bio-synthesized photonic crystals opened a new way towards innovative optically active nanostructures [10]. In parallel, the use of diatoms for their particular optical properties is a field of increasing interest [11-17]. These unicellular algae build complex bio-synthesized silica nanostructures called frustules. The special optical behavior of the frustules, including light focusing effects [13], has been shown to result from photonic crystal properties [15], which are suspected to help the diatoms enhancing their photosynthetic activity [11]. This work aims at developing a simple method to combine the complex nanostructure of diatom frustules with the plasmonic properties of gold NPs. Several methods can be used to generate gold NPs on a substrate. Chemical routes often involve surfactants limiting the coalescence of the gold NPs, but also providing some control over their shape [6,9]. However, surfactant molecules often interact with the surface of the gold NPs influencing their resulting LSPR properties. On the other hand, physical methods do not involve any stabilization at the surface of the gold NPs, hence giving less control over their shape.

The present study investigates two different methods using plasma sputtering to elaborate gold NPs at the surface of diatom frustules. The first method, based on the thermal dewetting of a gold layer, has already shown promising results on patterned substrates [18] and on one diatom species [10]. The second method involves the modification of the frustules surface using a coating of polyethylene glycol (PEG). Both methods are evaluated depending on the amount of gold sputtered on the frustules. The samples obtained from both methods are characterized by electron microscopy and the plasmonic properties of the gold NPs-decorated frustules are characterized by UV-visible spectroscopy.

EXPERIMENTAL SECTION

Clean diatom frustules of the *Coscinodiscus* species kept in methanol were used as substrates for gold deposition. Eight samples were prepared by drying droplets of a frustule-based dispersion on quartz substrates. Four samples were directly sputter coated with a layer of gold having a thickness of respectively 30 nm (sample 1), 20 nm (sample 2), 10 nm (sample 3) and 5 nm (sample 4). These four samples were then heated rapidly to 200 °C, then to 700 °C at a rate of 100 °C/min, maintained at 700 °C for 20 min, and finally cooled down rapidly. The four other samples were first coated with polyethylene glycol 400 (PEG 400) by depositing a droplet of PEG 400 aqueous solution (10^{-4} mol.L^{-1}) on the frustules. The samples were then dried and coated with a gold layer having a thickness of respectively 30 nm (sample 5), 20 nm (sample 6), 10 nm (sample 7) and 5 nm (sample 8).

Gold coatings were realized using a Cressington 208 HR sputter coater featuring a thickness controller. The thermal treatment was done using a Jipelec JetFirst 200 Rapid Thermal Processing (RTP) furnace under nitrogen flow. The observation of the gold layer was carried out using a Zeiss Ultra 55 FE-SEM operated at 15 kV. The TEM observations were realized using a JEOL 2010F operated at 200 kV. The UV-visible characterization was performed on a film of diatom frustules in diffuse reflection using an Avantes AvaSpec 2048 spectrometer featuring an integrative sphere.

RESULTS AND DISCUSSION

The *Coscinodiscus* diatom frustules are made of distinct parts: two valves joined by girdle bands, the valves showing a complex flower-like pattern of nanopores (see figure 1). The nanoporous valves are taken as the reference substrate of the gold deposition experiments.

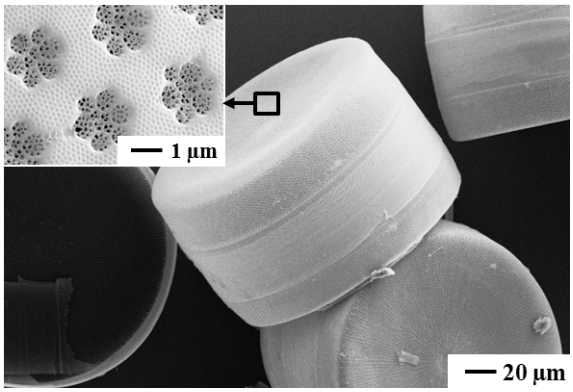

Figure 1. SEM micrographs of *Coscinodiscus* frustules.

The comparison of the samples prepared by the thermal dewetting method highlights a strong influence of the amount of sputtered gold on the resulting gold particles (see figure 2). The differences lie both in the particles mean size and in their size distribution. The thermal dewetting of a 30 nm thick gold layer (sample 1) results in a large dispersion of the particles size. Particles with a size up to 1.5 µm and down to 20 nm are observed (see figure 2.1). Sample 2, elaborated from a 20 nm thick gold layer, clearly features two families of gold NPs: large NPs with sizes ranging from 300 to 750 nm, and smaller NPs with sizes ranging from 9 to about

50 nm. All the large NPs seem well separated whereas the smaller NPs often appear agglomerated and coalesced, giving rise to larger complex structures (see figure 2.2). The thermal dewetting of a 10 nm thick gold layer (sample 3) highlights a very different result compared to the two previous samples. The gold NPs appear both smaller and with a narrower dispersion in size. No particle above 200 nm can be observed, but some coalescence between the NPs still leads to structures exceeding this size. In spite of a small area where the detachment of the gold layer can be observed, this layer looks very uniform all over the surface of the frustule. The frustule topography also seems to influence the gold layer as partially coalesced NPs can be observed at the edges of the valve pores, while separate gold NPs are observed elsewhere (see figure 2.3). Finally, the thermal dewetting of a 5 nm thick gold layer (sample 4) gives the smallest gold NPs with the most narrow distribution in size. In this sample, the frustules are evenly covered by a layer of gold NPs with a size below 50 nm (see figure 2.4).

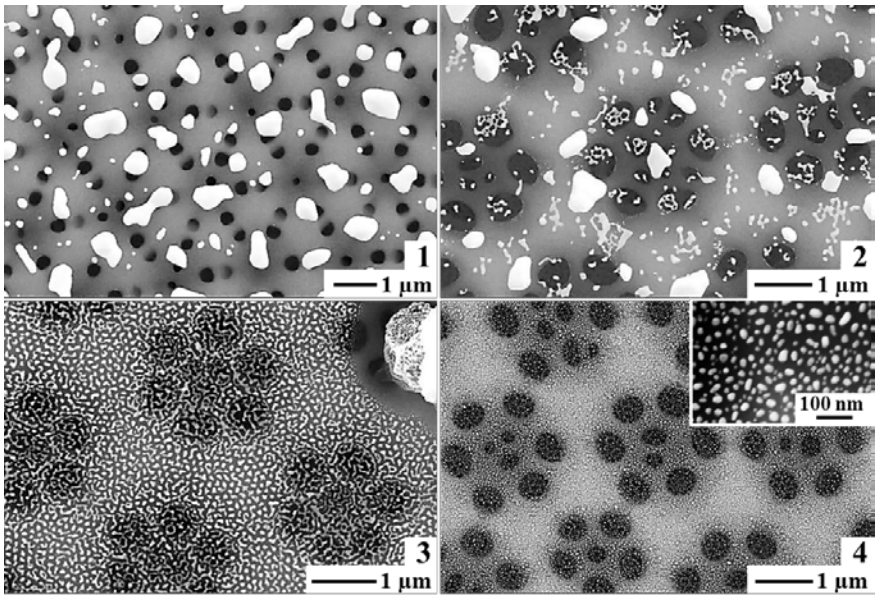

Figure 2. SEM micrographs of frustules featuring gold particles generated by thermal dewetting of a gold layer with a thickness of respectively 30 nm (1), 20 nm (2), 10 nm (3) and 5 nm (4).

A summary of the gold NPs size analysis for samples 1 to 4 is provided in table 1.

	Sample 1	Sample 2	Sample 3	Sample 4
Thickness of the sputtered layer [nm]	30	20	10	5
Particle mean size [nm]	367	110	84	19
Standard deviation [nm]	284	116	66	9

Table1. Particle size analysis of gold NPs found on the samples treated by thermal dewetting.

Sample 4 was observed more closely by TEM (see figure 3). The TEM images confirm the presence of gold NPs covering the frustules. In addition to a relatively narrow size distribution, no agglomeration could be observed. Gold NPs are present both between the frustule pores and on the thin silica branches inside the smallest pores. The particle size analysis from the TEM pictures indicate a mean size of 19.5 nm and a standard deviation of 9 nm, which is in good agreement with the observations from the SEM images.

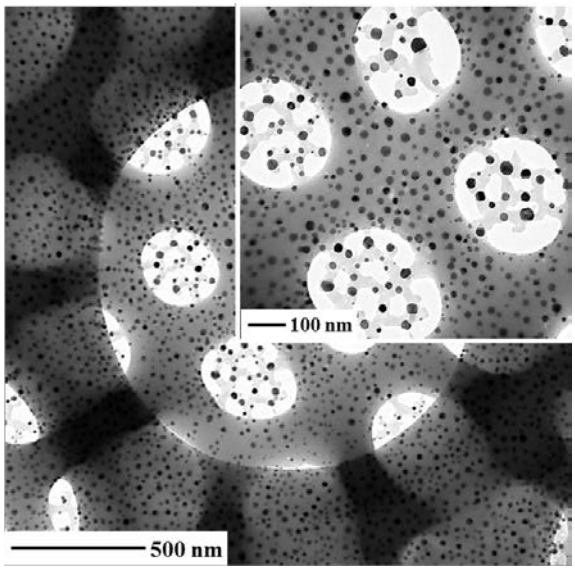

Figure 3. TEM micrographs of a frustule featuring gold NPs generated by thermal dewetting of a 5 nm thick gold layer.

The samples elaborated with the second method look quite different from the first four samples (see figure 4). Sputtering a 30 nm thick layer of gold on the PEG-coated frustules (sample 5) leads to a continuous layer of gold (see figure 4.5). At this point, the coating of PEG does not seem to have much effect on the gold coating process. A continuous layer is also observed when sputtering a 20 nm thick layer of gold on the PEG-coated frustules (sample 6). This layer seems smoother than in sample 5, and cracks are present over the frustule pores (see figure 4.6). The gold layer in sample 7 exhibits a different structure compared to samples 5 and 6. With 10 nm of sputtered gold, the obtained gold layer features evenly distributed nano-cavities with various shapes (see figure 4.7). This nanostructure corresponds to a dense network of coalesced NPs just above the percolation threshold. Finally, sputtering only 5 nm of gold leads to frustules evenly covered by gold NPs having sizes below 50 nm (sample 8), similarly to what is obtained in sample 4 by thermal dewetting (see figure 4.8). However, a difference in the mean size of the gold NPs is observed depending on the considered area, as the largest particles are mostly found between the pores, away from the pore edges. The mean particle size determined from a large area in sample 8 is 22 nm and the standard dispersion is 6 nm. If the areas including the pores are excluded, the mean particle size is 26 nm. When only considering the areas containing the pores, the mean size of the gold NPs is 15 nm, with several particles as small as 5 nm.

The samples obtained by the two methods show similarities for low amounts of sputtered gold (5 and 10 nm). Samples 3 and 7 both feature a nanostructured gold layer around the percolation threshold of gold NPs. Also samples 4 and 8 are similar regarding the NPs mean sizes (19 nm and 22 nm respectively). Nevertheless, only sample 8 seem to show a dependence between the size of the gold NPs and their location relatively to the pores.

The plasmonic activities of gold coated frustules (smooth gold layer obtained without any thermal dewetting treatment or PEG coating), sample 4 and sample 8 are compared by UV-visible spectroscopy (see figure 5).

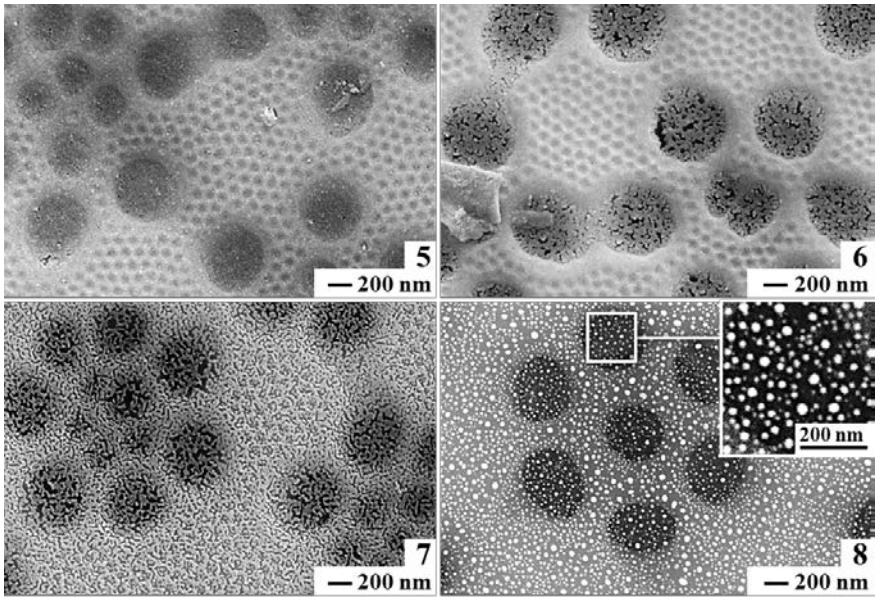

Figure 4. SEM micrographs of frustules featuring a coating of PEG under a plasma sputtered layer of gold with a thickness of respectively 30 nm (5), 20 nm (6), 10 nm (7) and 5 nm (8).

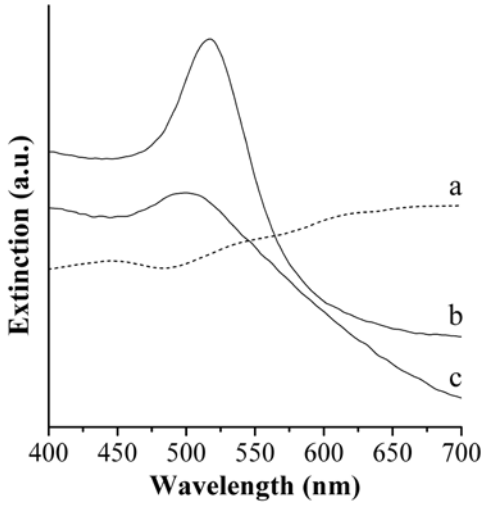

Figure 5. Extinction spectra of gold coated frustules (a), sample 4 (b) and sample 8 (c).

Since the sputter coating of frustules with gold results in a smooth gold layer, gold coated frustules do not show any extinction band between 400 and 700 nm (see figure 5a). The analysis of sample 4 shows a well-defined extinction band at 517 nm (see figure 5b). This extinction band is attributed to the LSPR of gold NPs with a typical size below 25 nm [1,19], which is in good agreement with the mean size of the gold NPs reported in table 1. Finally, sample 8 shows a weaker and broader extinction band centered at 502 nm (see figure 5c), which is much lower than what is expected from gold NPs having a mean size of 22 nm. As the PEG itself is not thought to alter the surface of the gold NPs, this result may suggest a greater influence of areas containing gold NPs smaller than 20 nm. Since electron microscopy indicates smaller gold NPs (around 15 nm) inside the pores and at the pores edges, it could mean that these areas have a stronger influence on the optical properties than the areas located away from the pores.

CONCLUSIONS

Bio-silica nanostructures combining photonic crystal and plasmonic properties can be elaborated from the plasma sputtering of gold on diatom frustules. The amount of sputtered gold is a significant parameter for both the thermal dewetting and the PEG coating methods regarding the size and the size distribution of the gold NPs. Both methods allow obtaining individual gold NPs of about 20 nm with a narrow size distribution at the surface of the frustules, but the PEG coating method seems to induce smaller NPs around and inside the pores. The two studied methods lead to an extinction band arising from the LSPR of the gold NPs at the frustules surface. The blue shift observed for the PEG-coated frustules may suggest the particular importance of the areas containing the pores regarding the resulting optical properties.

ACKNOWLEDGMENTS

The authors would like to thank Gabriella Tranell for her lead in this project, Matilde Chauton and Olav Vadstein for providing the frustules, Per Erik Vullum for obtaining the TEM images. Research supported by the Research Council of Norway (contract No.10358700).

REFERENCES

1. V.Amendola, M.Meneghetti, J. Phys. Chem. C 113, 4277 (2009)
2. M.Bosman, V.J.Keast, M.Watanabe, A.I.Maaroof, M.B.Cortie, Nanotechnol. 18, 165505 (2007)
3. M.B.Cortie, N.Stokes, A.McDonagh, Photonic Nanostruct. 7, 143 (2009)
4. J.A.Dionne, H.A.Atwater, MRS Bulletin 37 August 2012, 717 (2012)
5. C.Girard, E.Dujardin, G.Baffou, R.Quidant, New J. Phys. 10, 105016 (2008)
6. E.Hutter, J.H.Fendler, Adv. Mater. 16, 1685 (2004)
7. K.Nomura, Y.Ohki, M.Fujimaki, X.Wang, K.Awazu, T.Komatsubara, Nanotechnol. 20, 475306 (2009)
8. T.C.Petersen, M.Bosman, V.J.Keast, G.R.Anstis, Appl. Phys. Lett. 93, 101909 (2008)
9. V.Sharma, K.Park, M.Srinivasarao, Mater. Sci. Eng. R 65, 1 (2009)
10. M.P.Andrews, A.Hajiaboli, J.Hiltz, T.Gonzalez, G.Singh, R.B.Lennox, Proc. SPIE 7946, 79461S (2011)
11. R.Gordon, D.Losic, M.A.Tiffany, S.S.Nagy, F.A.S.Sterrenburg, Trends Biotechnol. 27-2, 116 (2008)
12. D.Losic, J.G.Mitchell, N.H.Voelcker, Adv. Mater. 21, 2947 (2009)
13. L.De Stefano, I.Rea, I.Rendina, M.De Stefano, L.Moretti, Opt. Express 15-26, 18082 (2007)
14. L.De Stefano, L.Rotiroti, M.De Stefano, A.Lamberti, S.Lettieri, A.Setaro, P.Maddalena, Biosens. Bioelectron. 24, 1580 (2008)
15. T.Fuhrmann, S.Landwehr, M.El Rharbi-Kucki, M.Sumper, Appl. Phys. B 78, 257 (2004)
16. E.De Tommasi, I.Rea, V.Mocella, L.Moretti, M.De Stefano, I.Rendina, L.De Stefano, Opt. Express 18-12, 12203 (2010)
17. P.Vukusic, J.R.Sambles, Nature 424, 852 (2003)
18. D.Wang, R.Ji, P.Schaaf, Beilstein J. Nanotechnol. 2, 318 (2011)
19. S.Link, M.El-Sayed, J. Phys. Chem. B 103, 4212 (1999)